



1 **Detecting small-scale spatial heterogeneity and temporal dynamics of soil organic carbon**
2 **(SOC) stocks: a comparison between automatic chamber-derived C budgets and repeated**
3 **soil inventories**

4

5 Mathias Hoffmann^{a,*}, Nicole Jurisch^b, Juana Garcia Alba^a, Elisa Albiac Borraz^a, Marten
6 Schmidt^b, Vytas Huth^b, Holger Rogasik^a, Helene Rieckh^a, Gernot Verch^c, Michael Sommer^{a, d},
7 Jürgen Augustin^b

8

9 ^aInstitute of Soil Landscape Research, Leibniz Centre for Agricultural Landscape Research
10 (ZALF), Eberswalder Str. 84, 15374 Müncheberg, Germany

11 ^bInstitute of Landscape Biogeochemistry, Leibniz Centre for Agricultural Landscape Research
12 (ZALF), Eberswalder Str. 84, 15374 Müncheberg, Germany

13 ^cResearch Station Dedelow, Leibniz Centre for Agricultural Landscape Research (ZALF),
14 Eberswalder Str. 84, 15374 Müncheberg, Germany

15 ^dInstitute of Earth and Environmental Sciences, University Potsdam, Karl-Liebknecht-Str.24-25,
16 14476 Potsdam, Germany

17

18 *Corresponding author:

19 Mathias Hoffmann

20 Eberswalder Str. 84, 15374 Müncheberg, Germany

21 E-mail: Mathias.Hoffmann@zalf.de

22 Tel.: +49(0)33432 82 327

23 Fax: +49(0)33432 82 280



24 Abstract

25 Carbon (C) sequestration in soils plays a key role in the global C cycle. It is therefore crucial to
26 adequately monitor dynamics in soil organic carbon (Δ SOC) stocks when aiming to reveal
27 underlying processes and potential drivers. However, small-scale spatial and temporal changes in
28 SOC stocks, particularly pronounced on arable lands, are hard to assess. The main reasons for
29 this are limitations of the well-established methods. On the one hand, repeated soil inventories,
30 often used in long-term field trials, reveal spatial patterns and trends in Δ SOC but require a
31 longer observation period and a sufficient number of repetitions. On the other hand, eddy
32 covariance measurements of C fluxes towards a complete C budget of the soil-plant-atmosphere
33 system may help to obtain temporal Δ SOC patterns but lack small-scale spatial resolution.

34 To overcome these limitations, this study presents a reliable method to detect both short-term
35 temporal as well as small-scale spatial dynamics of Δ SOC. Therefore, a combination of
36 automatic chamber (AC) measurements of CO_2 exchange and empirically modeled aboveground
37 biomass development ($\text{NPP}_{\text{shoot}}$) was used. To verify our method, results were compared with
38 Δ SOC observed by soil resampling.

39 AC measurements were performed from 2010 to 2014 under a *silage maize/winter fodder*
40 *rye/sorghum-Sudan grass hybrid/alfalfa* crop rotation at a colluvial depression located in the
41 hummocky ground moraine landscape of NE Germany. Widespread in large areas of the formerly
42 glaciated Northern Hemisphere, this depression type is characterized by a variable groundwater
43 level (GWL) and pronounced small-scale spatial heterogeneity in soil properties, such as SOC
44 and nitrogen (Nt). After monitoring the initial stage during 2010, soil erosion was experimentally
45 simulated by incorporating topsoil material from an eroded midslope soil into the plough layer of
46 the colluvial depression. SOC stocks were quantified before and after soil manipulation and at the
47 end of the study period.



48 AC-based Δ SOC values corresponded well with the tendencies and magnitude of the results
49 observed in the repeated soil inventory. The period of maximum plant growth was identified as
50 being most important for the development of spatial differences in annual Δ SOC. Hence, we
51 were able to confirm that AC-based C budgets are able to reveal small-scale spatial and short-
52 term temporal dynamics of Δ SOC.

53

54

55 **Keywords**

56 Net ecosystem exchange (NEE), net primary productivity (NPP), biomass modeling, soil
57 resampling

58



59 1. Introduction

60 Soils are the largest terrestrial reservoirs of organic carbon (SOC), storing two to three times as
61 much C as the atmosphere and biosphere (Chen et al., 2015; Lal et al., 2004). In the context of
62 climate change mitigation as well as soil fertility and food security, there has been considerable
63 interest in the development of SOC, especially in erosion-affected agricultural landscapes (Berhe
64 and Kleber, 2013; Conant et al., 2011; Doetterl et al., 2016; Stockmann et al., 2015; Van Oost et
65 al., 2007; Xiong et al., 2016). Detecting the development of soil organic carbon stocks (Δ SOC) in
66 agricultural landscapes needs to consider three major challenges: First, the high small-scale
67 spatial heterogeneity of SOC (e.g., Conant et al., 2010; Xiong et al., 2016). Erosion and land use
68 change reinforce natural spatial and temporal variability, especially in hilly landscapes such as
69 hummocky ground moraines where correlation lengths in soil parameters of 10-30 m are very
70 common. Second, pronounced short-term temporal dynamics, caused by, e.g., type of cover crop,
71 frequent crop rotation and soil cultivation practices. Third, the rather small magnitude of Δ SOC
72 compared to total SOC stocks (e.g., Conant et al., 2010; Poeplau et al., 2016).

73 However, information on the development of SOC is an essential precondition to improve the
74 predictive ability of terrestrial C models (Luo et al., 2014). As a result, sensitive measurement
75 techniques are required to precisely assess short-term temporal and small-scale spatial dynamics
76 in Δ SOC (Batjes and van Wesemael, 2015). To date, the assessment of Δ SOC is typically based
77 on two methods, namely (i) destructive, repeated soil inventories through soil resampling and (ii)
78 non-destructive determination of ecosystem C budgets by measurements of gaseous C exchange,
79 C import and C export (Leifeld et al., 2011).

80 The first method is usually used during long-term field trials (Batjes and van Wesemael, 2015;
81 Chen et al., 2015; Schrumpf et al., 2011). Given a sufficient time horizon of 5 to 10 years, the
82 soil resampling method is generally able to reveal spatial patterns and trends within Δ SOC



83 (Batjes and van Wesemael, 2015; Schrumpf et al., 2011). Most repeated soil inventories are
84 designed to study treatment differences in the long-term. As a result, short-term temporal
85 dynamics in C exchange remain concealed (Poeplau et al., 2016; Schrumpf et al., 2011). A
86 number of studies tried to overcome this methodical limitation by increasing (e.g., monthly) the
87 soil sampling frequency (Culman et al., 2013; Wuest, 2014). This allows for the detection of
88 seasonal patterns of Δ SOC but still mixes temporal and spatial variability of SOC because every
89 new soil sample represents not only a repetition in time but also in space. Temporal differences
90 observed through repeated soil sampling are therefore always spatially biased.

91 By contrast, temporal dynamics of Δ SOC can be easily derived through the eddy covariance (EC)
92 technique as a common approach to obtain gaseous C exchange (Alberti et al., 2010; Leifeld et
93 al., 2011; Skinner and Dell, 2015). However, C fluxes based on EC measurements are integrated
94 over a larger, altering footprint area (several hectares). As a result, small-scale (< 20 m) spatial
95 differences in Δ SOC are not detected.

96 Accounting for the above-mentioned methodical limitations, a number of studies investigated
97 spatial patterns in gaseous C exchange by using manual chamber measurement systems
98 (Eickenscheidt et al., 2014; Pohl et al., 2015). Compared to EC measurements, these systems are
99 characterized by a low temporal resolution, where the calculated net ecosystem CO₂ exchange
100 (NEE) is commonly based on extensive gap filling (Gomez-Casanovas et al., 2013; Savage and
101 Davidson, 2003) conducted, e.g., using empirical modeling (Hoffmann et al., 2015). Therefore,
102 management practices and different stages in plant development that are needed to precisely
103 detect NEE often remain unconsidered (Hoffmann et al., 2015). In contrast, automatic chamber
104 (AC) systems combine the advantages of EC and manual chamber systems because they increase
105 the temporal resolution compared to manual chambers but also allow for the detection of small-
106 scale spatial variability in gaseous C exchange (Koskinen et al., 2014).



107 Hardly any direct comparisons between AC-derived C budgets and soil resampling-based Δ SOC
108 values have been reported in the literature. Leifeld et al. (2011) and Verma et al. (2005)
109 compared the results of repeated soil inventories with EC-based C budgets over 5- and 3-year
110 study periods, respectively. Even though temporal dynamics in Δ SOC were shown (Leifeld et al.,
111 2011), no attempt was made to additionally detect small-scale differences in Δ SOC. In our study,
112 we introduce the combination of AC measurements and empirically modeled aboveground
113 biomass production (NPP_{shoot}) as a precise method to detect small-scale spatial and short-term
114 temporal dynamics of Δ SOC. Measurements were performed from 2010 to 2014 under a *silage*
115 *maize/winter fodder rye/sorghum-Sudan grass hybrid/alfalfa* crop rotation at an experimental plot
116 located in the hummocky ground moraine landscape of NE Germany.

117 We hypothesize that the AC-based C budget method is able to detect small-scale spatial and
118 short-term temporal dynamics of Δ SOC in an accurate and precise manner. Therefore, we
119 compare Δ SOC values measured by soil resampling with Δ SOC values derived through AC-
120 based C budgets (Fig. 1).

121

122 **2. Materials and methods**

123 **2.1 Study site and experimental setup**

124 Measurements were performed at the 6-ha experimental field “CarboZALF-D”. The site is
125 located in a hummocky arable soil landscape within the Uckermark region (NE-Germany;
126 53°23`N, 13°47`E, ~50-60 m a.s.l.). The temperate climate is characterized by a mean annual
127 temperature of 8.6°C and annual precipitation of 485 mm (1992–2012, ZALF research station,
128 Dedelow). Typical landscape elements vary from flat summit and depression locations with a
129 gradient of approximately 2 %, across longer slopes with a medium gradient of approx. 6 %, to
130 short and rather steep slopes with a gradient of up to 13 %. The study site shows complex soil



131 patterns mainly influenced by erosion, relief and parent material, e.g., sandy to marly glacial and
132 glaciofluvial deposits. The soil type inventory of the experimental site consists of non-eroded
133 Albic Luvisols (Cutanic) at the flat summits, strongly eroded Calcic Luvisols (Cutanic) on the
134 moderate slopes, extremely eroded Calcaric Regosols on the steep slopes, and a colluvial soil,
135 i.e., Endogleyic Colluvic Regosols (Eutric), over peat in the depression (IUSS Working Group
136 WRB, 2015).

137 During June 2010, four automatic chambers and a WXT520 climate station (Vaisala, Vantaa,
138 Finland) were set up at the depression (Sommer et al., 2016). The chambers were arranged along
139 a topographic gradient (upper (A), upper middle (B), lower middle (C), and lower (D) chamber
140 position; length ~30 m; difference in altitude ~1 m) within in a distance of approx. 5 m of each
141 other (Fig. 2). As part of the CarboZALF project, a manipulation experiment was carried out at
142 the end of October 2010, i.e., after the vegetation period. Topsoil material from a neighboring
143 hillslope was incorporated into the upper soil layer of the depression (Ap horizon). The amount
144 of translocated soil was equivalent to tillage erosion of a decennial time horizon (Sommer et al.,
145 2016). The change in SOC for each chamber was monitored by three topsoil inventories, carried
146 out (I) prior to soil manipulation during April 2009, (II) after soil manipulation during April
147 2011, and (III) during December 2014.

148 Records of meteorological conditions (1 min frequency) include measurements of air temperature
149 at 20 cm and 200 cm height, PAR (inside and outside the chamber), air humidity, precipitation,
150 air pressure, wind speed and direction. Soil temperatures at depths of 2 cm, 5 cm, 10 cm and 50
151 cm were recorded using thermocouples, installed next to the climate station (107, Campbell
152 Scientific, UT, USA).

153 The groundwater level (GWL) was measured using tensiometers assuming hydrostatic
154 equilibrium. The tensiometers were installed at a soil depth of 160 cm, at soil profile locations in



155 the upper and lower end of the transect. The average GWL of both profiles was used for further
156 data analysis. Data gaps < 2 days were filled using simple linear interpolation. Larger gaps in
157 GWL did not occur. The measurement site was cultivated under a silage maize (*Zea mays*) -
158 winter fodder rye (*Secale cereale*) - sorghum-Sudan grass hybrid (*Sorghum bicolor x sudanese*) -
159 winter triticale (*Triticosecale*) - alfalfa (*Medicago sativa*) crop rotation, following a practice-
160 orientated and erosion-expedited farming procedure. Cultivation and fertilization details are
161 presented in Tab. A.1. Aboveground biomass (NPP_{shoot}) development was monitored using up to
162 four biomass sampling campaigns during the growing season, covering the main growth stages.
163 Additional measurements of leaf area index (LAI) started in 2013. Collected biomass samples
164 were chopped and dried to a constant weight (48 h at 105°C). The C, N, K and P contents were
165 determined using elementary analysis (C, N: TruSpec CNS analyzer, LECO Ltd.,
166 Mönchengladbach, Germany) and Kjehldahl digestion (P, K; AT200, BeckmanCoulter
167 (Olympus), Krefeld, Germany and AAS-iCE3300, ThermoFisher-SCIENTIFIC GmbH,
168 Darmstadt, Germany). To assess the potential impact of chamber placement on plant growth,
169 chemical analyses were carried out for the final harvests of each chamber and compared to
170 biomass samples collected next to each chamber.

171

172 **2.2 C budget method**

173 **2.2.1 Automatic chamber system**

174 Automatic flow-through non-steady-state (FT-NSS) closed chamber measurements (Livingston
175 and Hutchinson, 1995) of CO₂ exchange were conducted from January 2010 until December
176 2014. The AC system consists of 4 identical, rectangular, transparent polycarbonate chambers
177 (thickness of 2 mm; light transmission ~70 %). Each chamber has a height of 2.5 m and covers a
178 surface area of 2.25 m² (volume: 5.625 m³). To adapt for plant height (alfalfa), the chamber



179 volume was reduced to 3.275 m³ in autumn 2013. Airtight closure during measurements was
180 ensured by a rubber belt that sealed at the bottom of each chamber. A 30-cm open-ended tube on
181 the slightly concave top of the chambers guided rain water into the chamber and additionally
182 assured pressure equalization. Two small axial fans (5.61 m³ min⁻¹) were used for mixing the
183 chamber headspace. The chambers were mounted onto steel frames with a height of 6 m and
184 lifted between measurements using electrical winches at the top. For controlling the AC system
185 and data collection, a CR1000 data logger was used (Campbell Scientific, UT, USA). For easy
186 access, the data logger was connected to a GSM-modem. The data logger and controlling device
187 were placed inside a weather-sheltered house next to the measurement site. CO₂ concentration
188 changes over time were measured within each chamber using a carbon dioxide probe (GMP343,
189 Vaisala, Vantaa, Finland) connected to a vacuum pump (1 l min⁻¹; DC12/16FK, Fürgut,
190 Tannheim, Germany). All CO₂ probes were calibrated prior to installation using ± 0.5 % accurate
191 gases containing 0 ppm, 200 ppm 370 ppm, 600 ppm, 1000, ppm and 4000 ppm CO₂. The
192 operation schedule of the AC system, decisively influenced by agricultural treatments, is
193 presented in A.2. The chambers closed in parallel at an hourly frequency, providing one flux
194 measurement per chamber and hour. The measurement duration was 5-20 minutes, depending on
195 season and time of day. Nighttime measurements usually lasted 10 min during the growing
196 season and 20 min during the non-growing season. The length of the daytime measurements was
197 up to 10 min, depending on low PAR fluctuations (< 20 %). CO₂ concentrations (inside the
198 chamber) and general environmental conditions, such as PAR (SKP215, Skye, Llandridad Wells,
199 UK) and air temperatures (107, Campbell Scientific, UT, USA), were recorded inside and outside
200 the chambers at a 1 min frequency from 2010 to 2012 and a 15 sec frequency from October 2012.

201

202 2.2.2 CO₂ flux calculation and gap filling



203 An adaptation of the modular R program script, described in detail by Hoffmann et al. (2015),
204 was used for stepwise data processing. The atmospheric sign convention was used for the
205 components of gaseous C exchange (ecosystem respiration (R_{eco}), gross primary production
206 (GPP) and NEE), whereas positive values for ΔSOC indicate a gain and negative values a loss in
207 SOC. Based on records of environmental variables and CO_2 concentration change within the
208 chamber headspace, CO_2 fluxes were calculated and parameterized for R_{eco} and GPP within an
209 integrative step. Subsequently, R_{eco} , GPP, and NEE were modeled for the entire measurement
210 period using climate station data. Statistical analyses, model calibration and comprehensive error
211 prediction were provided for all steps of the modeling process. CO_2 fluxes were calculated
212 according to the ideal gas law using chamber volume, basal area, within-chamber air temperature,
213 air pressure and CO_2 concentration records. Therefore, data subsets based on a variable moving
214 window with a minimum length of 4 minutes were used (Hoffmann et al., 2015). Because plants
215 below the chambers accounted for $< 0.2\%$ of the total chamber volume, a static chamber volume
216 was assumed. $\Delta c/\Delta t$ was computed by applying a linear regression, which estimated the flux by
217 using the least squares method to relate changes in chamber headspace CO_2 concentration (Δc) to
218 measurement time (Δt) (Leiber-Sauheitl et al., 2013; Leifeld et al., 2014; Pohl et al., 2015). In the
219 case of the 15-sec measurement frequency, a death-band of 5 % was applied prior to the moving
220 window algorithm. Thus, data noise that originated from either turbulence or pressure fluctuation
221 caused by chamber deployment or from increasing saturation and canopy microclimate effects
222 was excluded (Davidson et al., 2002; Kutzbach et al., 2007; Langensiepen et al., 2012). Due to
223 the low measurement frequency, no data points were discarded for records with 1-min
224 measurement frequency (2010-2012). The resulting CO_2 fluxes per measurement (based on the
225 moving window data subsets) were further evaluated according to the following exclusion
226 criteria: (i) range of within-chamber air temperature not larger than $\pm 1.5\text{ K}$ (R_{eco} and NEE



227 fluxes) and a PAR deviation (NEE fluxes only) not larger than $\pm 20\%$ of the average to ensure
 228 stable environmental conditions within the chamber throughout the measurement; (ii) significant
 229 regression slope ($p \leq 0.1$, t -test); and (iii) non-significant tests ($p > 0.1$) for normality (Lillifor's
 230 adaption of the Kolmogorov-Smirnov test), homoscedasticity (Breusch-Pagan test) and linearity
 231 of CO₂ concentration data as suggested by. Calculated CO₂ fluxes that did not meet all exclusion
 232 criteria were discarded. In cases where more than one flux per measurement met all exclusion
 233 criteria, the CO₂ flux with the steepest slope was chosen.

234 To account for measurement gaps and to obtain cumulative NEE values, empirical models were
 235 derived based on nighttime R_{eco} and daytime NEE measurements following Hoffmann et al.
 236 (2015). For R_{eco} , temperature-dependent Arrhenius-type models were used (Lloyd and Taylor
 237 1994; Eq. 1).

238

$$239 \quad R_{eco} = R_{ref} * e^{E_0 \left(\frac{1}{T_{ref}-T_0} - \frac{1}{T-T_0} \right)} \quad [Eq. 1]$$

240

241 where R_{eco} is the measured ecosystem respiration rate [$\mu\text{mol}^{-1} \text{m}^{-2} \text{s}^{-1}$], R_{ref} is the respiration rate
 242 at the reference temperature (283.15 K; T_{ref}); E_0 is an activation energy like parameter; T_0 is the
 243 starting temperature constant (227.13 K) and T is the mean temperature during the flux
 244 measurement. GPP fluxes were derived using a PAR-dependent, rectangular hyperbolic light
 245 response function based on the Michaelis-Menten kinetic (Elsgaard et al., 2012; Hoffmann et al.,
 246 2015; Wang et al., 2013; Eq. 2). Because GPP was not measured directly, GPP fluxes were
 247 calculated as the difference between measured NEE and modeled R_{eco} fluxes.

248

$$249 \quad GPP = \frac{GP_{max} * \alpha * PAR}{\alpha * PAR + GP_{max}} \quad [Eq. 2]$$



250

251 where GPP is the calculated gross primary productivity [$\mu\text{mol}^{-1} \text{CO}_2 \text{ m}^{-2} \text{ s}^{-1}$]; GP_{max} is the
 252 maximum rate of C fixation at infinite PAR [$\mu\text{mol CO}_2 \text{ m}^{-2} \text{ s}^{-1}$]; α is the light use efficiency [mol
 253 $\text{CO}_2 \text{ mol}^{-1}$ photons] and PAR is the photon flux density (inside the chamber) of the
 254 photosynthetically active radiation [μmol^{-1} photons $\text{m}^{-2} \text{ s}^{-1}$]. In cases where the rectangular
 255 hyperbolic light response function did not result in significant parameter estimates, a non-
 256 rectangular hyperbolic light-response function was used (Gilmanov et al. 2007, 2013; Eq. 3).

257

$$258 \quad GPP = \alpha * PAR + GP_{max} - \sqrt{(\alpha * PAR + GP_{max})^2 - 4 * \alpha * PAR * GP_{max} * \theta} \quad [\text{Eq. 3}]$$

259

260 where θ is the convexity coefficient of the light-response equation (dimensionless).

261 Due to plant growth and season, parameters of derived R_{eco} and GPP models may vary with time.

262 To account for this, a moving window parameterization was performed, by applying fluxes of a
 263 variable time window (2-21 consecutive measurement days) to Eq.1-3. Temporally overlapping
 264 R_{eco} and GPP model sets were evaluated and discarded in case of positive (GPP), negative (Reco)
 265 or insignificant parameter estimates. Finally, the model set with the lowest Akaike Information
 266 Criterion (AIC; R_{eco}) was used. If no fit or a non-significant fit was achieved, averaged flux rates
 267 were applied for R_{eco} and GPP. The length of the averaging period was thereby selected by
 268 choosing the variable moving window with the lowest standard deviation (SD) of measured
 269 fluxes. This procedure was repeated until the whole study period was parameterized.

270 Based on continuously monitored temperature and PAR (outside the chamber), R_{eco} , GPP and

271 NEE were modeled in half-hour steps for the entire study period. Because GPP was

272 parameterized based on PAR records inside but modeled with PAR records outside the chamber,

273 no PAR correction in terms of reduced light transmission was needed. Uncertainty of annual CO_2



274 exchange was quantified using a comprehensive error prediction algorithm described in detail by
275 Hoffmann et al. (2015).

276

277 **2.2.3 Modeling aboveground biomass dynamics**

278 Aboveground biomass development (NPP_{shoot}) was predicted using a logistic empirical model.
279 From 2010 to 2012, modeled NPP_{shoot} was based on the relationship between sampling date and
280 the C content of harvested dry biomass measured during sampling campaigns (three to four times
281 per year following plant development) (Yin et al., 2003; Zeide, 1993). For alfalfa in 2013 and
282 2014, NPP_{shoot} was modeled based on biweekly measurements of LAI because no additional
283 biomass sampling was performed between the multiple cuts per year. To calculate the C content
284 corresponding to the measured LAI, the relationship between LAI prior to the chamber harvest
285 and the C content measured in the chamber harvest of all six alfalfa cuts was used. Daily values
286 of C stored within NPP_{shoot} were calculated using derived logistic functions.

287

288 **2.2.4 Calculation of ΔSOC**

289 Annual ΔSOC for each chamber was determined as the sum of annual NEE and NPP_{shoot} ,
290 representing C removal due to the chamber harvest (Eq. 4; Leifeld et al., 2014). Temporal
291 dynamics in ΔSOC were calculated as the sum of daily NEE and NPP_{shoot} .

292

$$293 \quad \Delta SOC_n = \sum_{i=1}^n [NEE_i + NPP_{shoot_i}] \quad [\text{Eq. 4}]$$

294

295 Several minor components were not considered in Eq. 4 (see also Hernandez-Ramirez et al.,
296 2011). First, C import (C_{in}) due to seeding and fertilization, which was close to zero because the
297 measurement site was fertilized by a surface application of mineral fertilizer throughout the entire



298 study period. Second, methane ($\text{CH}_4\text{-C}$) emissions, which were measured manually at the same
299 experimental field but did not exceed a relevant order of magnitude and were therefore not
300 included in the ΔSOC calculation. Third, lateral C fluxes, originating from dissolved organic
301 (DOC) and inorganic carbon (DIC) as well as particulate soil organic carbon (SOC_p). In addition
302 to the rather small magnitude of the subsurface lateral C fluxes in soil solution (Rieckh et al.,
303 2012), it was assumed that their C input equaled C output at the plot scale. Lateral SOC_p
304 transport along the hillslope was excluded by grassland stripes established between experimental
305 plots in 2010 (Fig. 1 in Sommer et al., 2016).

306

307 **2.3 Soil resampling method**

308 To obtain ΔSOC using the soil resampling method, soil samples were collected three times
309 during the study period. Initial SOC along the topographic gradient was monitored prior to soil
310 manipulation during April 2009 at two soil pits, which were sampled by pedogenetic horizons.
311 After soil manipulation, a 5-m raster sampling of the Ap horizons (once for the upper and once
312 for the lower Ap horizon) was performed during April 2011. Specifically, undisturbed soil cores
313 were collected using 5 steel rings (each 100 cm^3) per horizon. In December 2014, mixed soil
314 samples were collected from the Ap horizon next to each chamber. Thermogravimetric
315 desiccation at 105°C was performed in the laboratory for all samples to determine bulk densities
316 (Mg m^{-3}). Bulk soil samples were air dried, gently crushed and sieved (2 mm) to obtain the fine
317 fraction (particle size $< 2\text{ mm}$). The total carbon and total nitrogen contents were determined by
318 elementary analysis (TruSpec CNS analyzer, LECO Ltd., Mönchengladbach, Germany) as
319 carbon dioxide via infrared detection after dry combustion at 1250°C (DIN ISO10694, 1996), in
320 duplicate. As the soil horizons did not contain carbonates, total carbon was equal to SOC.

321



322 **2.4 Uncertainty prediction and statistical analysis**

323 Uncertainty prediction for Δ SOC derived by the C budget method was performed according to
324 Hoffmann et al. (2015), following the law of error propagation. To test for differences in topsoil
325 SOC (SOC_{Ap}) and total nitrogen (Nt) stocks between soil resampling performed after soil
326 manipulation in 2010 and 2014, a paired *t*-test was applied. Computation of uncertainty
327 prediction and calculation of statistical analyses were performed using R 3.2.2.

328

329 **3. Results**

330 **3.1 C budget method**

331 **3.1.1 NEE and $\text{NPP}_{\text{shoot}}$ dynamics**

332 NEE and its components R_{eco} and GPP were characterized by a clear seasonality, following plant
333 growth and management events (e.g., harvest; Fig. 3). Highest CO_2 uptake was thus observed
334 during the growing season, whereas NEE fluxes during the non-growing season were
335 significantly lower. Annual NEE was crop dependent, ranging from $-1600 \text{ g C m}^{-2} \text{ a}^{-1}$ to -288 g C
336 $\text{m}^{-2} \text{ a}^{-1}$. Highest annual uptakes were observed for maize and sorghum during 2011 and 2012,
337 whereas alfalfa cultivation showed lower annual NEE (Tab. 1). From 2010 to 2012, annual NEE
338 followed the topographic gradient, with higher NEE in the direction of the depression and lower
339 NEE away from the depression. This small-scale spatial heterogeneity in gaseous C exchange
340 changed with alfalfa cultivation. As a result, only minor differences between the chamber
341 positions were observed, showing no clear trend or tendency (Tab. 1).

342 C in living biomass (due to biomass sampling campaigns and LAI measurements) and C
343 removals due to harvest were in general well reflected by modeled $\text{NPP}_{\text{shoot}}$ (Fig. 4). Annual C
344 removal due to harvest was clearly crop dependent, with highest $\text{NPP}_{\text{shoot}}$ for maize and sorghum
345 ranging from 420 g C m^{-2} to 1238 g C m^{-2} , and lower values in the case of winter fodder rye and



346 alfalfa. Similar to NEE from 2010 to 2012, annual sums of NPP_{shoot} followed the topographic
347 gradient, with lower values close to the depression (Tab. 1). Again, lower differences in annual
348 NPP_{shoot} between chamber positions and no spatial trends were found for alfalfa in 2013 and
349 2014.

350

351 **3.1.2 Δ SOC dynamics**

352 Temporal and spatial dynamics of continuously cumulated daily Δ SOC values during the four
353 years after soil manipulation are shown in Fig. 5. Differences in Δ SOC were in general less
354 pronounced during the non-growing season compared to the growing season. During the non-
355 growing season, differences were mainly driven by differences in R_{eco} rather than GPP or
356 NPP_{shoot} . This changed at the beginning of the growing season, when Δ SOC responded to
357 changes in cumulative NEE and NPP_{shoot} . Hence, up to 79 % of the standard deviation of
358 estimated annual Δ SOC developed during the period of maximum plant growth. Except for the
359 lower middle chamber position, alfalfa seemed to counterbalance spatial differences in Δ SOC
360 that developed during previous years (Fig. 5).

361 Annual Δ SOC values derived by the C budget method are presented in Tab. 1. Highest annual
362 SOC gains were obtained in 2012 for winter fodder rye and sorghum-Sudan grass, reaching an
363 average of $474 \text{ g C m}^{-2} \text{ a}^{-1}$. In contrast, maize cultivation during 2011 was characterized by C
364 losses between $59 \text{ g C m}^{-2} \text{ a}^{-1}$ and $169 \text{ g C m}^{-2} \text{ a}^{-1}$. However, prior to soil manipulation, maize
365 showed an average SOC gain of $102 \text{ g C m}^{-2} \text{ a}^{-1}$.

366

367 **3.2 Soil resampling method**

368 As a result of soil translocation in 2010, initially measured SOC_{Ap} stocks increased by an average
369 of 780 g C m^{-2} . However, due to the lower C content of the translocated topsoil material (0.76



370 %), the SOC_{AP} content of the measurement site dropped by 10 - 14 % after soil manipulation
371 (Tab. 1). Significant differences (paired t -test; $t = -2.48$, $p < 0.09$), which showed an increase in
372 SOC_{AP} of up to 11 %, were found between SOC_{AP} stocks measured in 2010 and 2014. Three out
373 of the four chamber positions showed a C gain during the 4 measurement years following soil
374 manipulation. C gains were similar for the upper and lower chamber positions, but lower for the
375 upper middle position. No change in SOC was obtained in the case of the lower middle (Fig. 5;
376 Fig. 6) chamber position.

377

378 **3.3 Method comparison**

379 Average annual ΔSOC values for the soil resampling and C budget method are shown in Fig. 6.
380 ΔSOC based on these methods showed a good overall agreement, with similar tendencies and
381 magnitudes (Fig. 6). Irrespective of the applied method, significant differences were found
382 between SOC stocks measured directly after soil manipulation in 2010 and SOC stocks measured
383 in 2014. Following soil manipulation, both methods revealed similar tendencies in site and
384 chamber-specific ΔSOC (Fig. 6). Both methods indicated a clear C gain for three out of the four
385 chamber positions. C gains derived by the C budget method were similar for the upper, upper
386 middle and lower chamber positions. By contrast, C gains derived by the soil resampling method
387 were slightly but not significantly lower (paired t -test; $t = -1.23$, $p > 0.30$). This was most
388 pronounced for the upper middle chamber position. No change in ΔSOC and only a minor gain in
389 C was observed for the lower middle chamber position according to both methods. Differences
390 between chamber positions indicate the presence of small-scale spatial ΔSOC dynamics typical of
391 soils (Conant et al., 2010; Xiong et al., 2016).

392

393 **4. Discussion**



394 **4.1 Accuracy and precision of applied methods**

395 Despite the similar magnitude and tendencies of the observed Δ SOC values, both methods were
396 subject to numerous sources of uncertainty. These errors affect the accuracy and precision of
397 observed Δ SOC values differently, which might help to explain differences between the soil
398 resampling and the C budget method.

399 The soil resampling method is characterized by high measurement precision, which allows for the
400 detection of relatively small changes in SOC. Related uncertainty in derived spatial and temporal
401 Δ SOC dynamics is therefore mainly attributed to the measurement accuracy, affected by
402 sampling strategy and design (Batjes and van Wesemael, 2015; De Gruijter et al., 2006). This
403 includes (i) the spatial distribution of collected samples, (ii) the sampling frequency, (iii) the
404 sampling depth and (iv) whether different components of soil organic matter (SOM) are excluded
405 prior to analyses. The first aspect determines the capability to detect the inherent spatial
406 variability in SOC stocks. This allows the conclusion that point measurements do not necessarily
407 represent AC measurements, which integrate over the spatial variability within their basal area.
408 The second aspect defines the temporal resolution, even though the soil resampling method is not
409 able to perfectly separate spatial from temporal variability because repeated soil samples are
410 biased by inherent spatial variability of the measurement site. The third aspect sets the vertical
411 system boundary, which is often limited because only topsoil horizons are sampled within a
412 number of soil monitoring networks (Van Wesemael et al., 2011) and repeated soil inventories
413 (Leifeld et al., 2011). Similarly, the fourth aspect defines which components of SOM are
414 specifically analyzed. Usually, coarse organic material is discarded prior to analysis (Schlichting
415 et al., 1995) and therefore, total SOC is not assessed (e.g., roots, harvest residues, etc.).

416 In comparison, the C budget method considers any type of organic material present in soil by
417 integrating over the total soil depth. As a result, both methods have a different validity range and



418 area, which makes direct quantitative comparison more difficult. This may explain the higher
419 uptake reported for three out of four chamber positions in the case of the C budget method.

420 In contrast to the soil resampling method, we postulate a higher accuracy and a lower precision in
421 the case of the AC-based C budget method. The reasons for this include a number of potential
422 errors affecting especially the measurement precision of the AC system, whereas over a constant
423 area and maximum soil depth, integrated AC measurements increase measurement accuracy.

424 First, it is currently not clear whether microclimatological and ecophysiological disturbances due
425 to chamber deployment, such as the alteration of temperature, humidity, pressure, radiation, and
426 gas concentration, may result in biased C flux rate estimates (Juszczak et al., 2013; Kutzbach et
427 al., 2007; Lai et al., 2012; Langensiepen et al., 2012). Second, uncertainties related to performed
428 flux separation and gap-filling procedures may influence the obtained annual gaseous C exchange
429 (Gomez-Casanovas et al., 2013; Görres et al., 2014; Moffat et al., 2007; Reichstein et al., 2005).

430 Although continuous operation of the AC system should allow for direct derivation of C budgets
431 from measured CO₂ exchange and annual yields, in practice, data gaps always occur. To fill the
432 measurement gaps, temperature- and PAR-dependent models are derived and used to calculate
433 R_{eco} and GPP, respectively. Due to the transparent chambers used, modeled R_{eco} is solely based
434 on nighttime measurements. Hence, systematic differences between nighttime and daytime R_{eco}
435 will yield an over- or underestimation of modeled R_{eco}. Because modeled R_{eco} is used to calculate
436 GPP fluxes, GPP will be affected in a similar manner. However, the systematic over- or
437 underestimation of fluxes in both directions may counterbalance the computed NEE, and
438 estimated C budgets may be unaffected. Third, the development of NPP_{shoot} underneath the
439 chamber might be influenced by the permanently installed AC system. Fourth, several minor
440 components such as leaching losses of dissolved inorganic and organic carbon (DIC and DOC),



441 C transport via runoff and atmospheric C deposition were not considered within the applied
442 budgeting approach (see also 2.7).

443 Despite the uncertainties mentioned above, error estimates for annual NEE in this study are
444 within the range of errors presented for annual NEE estimates derived from EC measurements
445 (30 to $50 \text{ g C m}^{-2} \text{ a}^{-1}$) (e.g., Baldocchi, 2003; Dobermann et al., 2006; Hollinger et al., 2005) and
446 below the minimum detectable difference (MDD) reported for most repeated soil inventories
447 (e.g., Batjes and Van Wesemael, 2015; Knebl et al., 2015; Nécipálová et al., 2014; Saby et al.,
448 2008; Schrumpf et al., 2011; VandenBygaart, 2006).

449

450 **4.2 Plausibility of observed ΔSOC**

451 Both the soil resampling and the C budget method showed C gains during the four years
452 following soil manipulation. A number of authors calculated additional C sequestration due to
453 soil erosion (Berhe et al., 2007; Dymond, 2010; VandenBygaart et al., 2015; Yoo et al., 2005),
454 which was explained by the burial of replaced C at depositional sites and dynamic replacement at
455 eroded sites (e.g., Doetterl et al., 2016). This is in accordance with erosion-induced C
456 sequestration postulated by, e.g., Berhe and Kleber (2013) and Van Oost et al. (2007). In
457 addition, observed C sequestration could also be a result of the manipulation-induced saturation
458 deficit in SOC. By adding topsoil material from an eroded unsaturated hillslope soil, the capacity
459 and efficiency to sequester C was theoretically increased (Stewart et al., 2007). Hence, additional
460 C was stored at the measurement site. This might be due to physicochemical processes, such as
461 physical protection in macro- and micro aggregates (Six et al., 2002) or chemical stabilization by
462 clay and iron minerals (Kleber et al., 2015).

463 Irrespective of the similar C gain observed by both methods, crop-dependent differences in
464 ΔSOC were only revealed by the C budget method. The reason is the higher temporal resolution



465 of AC-derived C budgets, displaying daily C losses and gains. Observed crop-dependent
466 differences in Δ SOC are in accordance with, e.g., Kutsch et al. (2010), Jans et al. (2010),
467 Hollinger et al. (2005) and Verma et al. (2005), who reported comparable EC-derived C balances
468 for inter alia, maize, sorghum and alfalfa.

469 In 2012, substantial positive annual Δ SOC values were observed. Due to low precipitation during
470 May and June, germination and plant growth of sorghum-Sudan grass was delayed (Fig. 4). As a
471 result, the reproductive phenological stage was drastically shortened. This reduced C losses prior
472 to harvest due to higher R_{eco} :GPP ratios (Wagle et al., 2015). In addition, the presence of cover
473 crops during spring and autumn could have increased SOC, as reported by Lal et al. (2004),
474 Ghimire et al. (2014) and Sainju et al. (2002). No additional C sequestration was observed for
475 alfalfa in 2013 and 2014 or for the lower middle chamber position, which acted neither as a net C
476 source nor sink (Tab. 1; Fig. 5). This opposes the assumption of increased C sequestration by
477 perennial grasses (Paustian et al., 1997) or perennial crops (Zan et al., 2001). However, NEE
478 estimates of alfalfa were within the range of -100 to -400 g C m⁻², which is typical for forage
479 crops (*Lolium*, alfalfa, etc.) in different agro-ecosystems (Bolinder et al., 2012; Byrne et al.,
480 2005; Gilmanov et al., 2013; Zan et al., 2001). In addition, Alberti et al. (2010) reported a soil C
481 loss of > 170 g C m⁻² after crop conversion from continuous maize to alfalfa, concluding that no
482 effective C sequestration occurs in the short-term.

483 Regardless of the crop type, the AC-derived dynamic Δ SOC values showed that up to 79 % of
484 the standard deviation of estimated annual Δ SOC occurred during the growing season and the
485 main plant growth period from the beginning of July to the end of September.

486

487 5. Conclusions



488 We confirmed that AC-based C budgets are able to reveal small-scale spatial and short-term
489 temporal dynamics of Δ SOC. AC-derived C budgets showed not only pedon-scale differences but
490 also pronounced temporal dynamics in Δ SOC (Fig. 5). In addition, AC-based Δ SOC values
491 corresponded well with the tendencies and magnitude of the results observed in the repeated soil
492 inventory. The period of maximum plant growth was identified as being most important for the
493 development of spatial differences in annual Δ SOC. For upscaling purposes of the presented
494 results, further environmental drivers, processes and mechanisms determining C allocation in
495 space and time within the plant-soil system need to be identified. This type of an approach will be
496 pursued in future within the CarboZALF experimental setup (Sommer et al., 2016; Wehrhan et
497 al., 2016). Moreover, the AC-based C budget method opens new prospects for clarifying
498 unanswered questions, such as the influence of plant development or erosion on Δ SOC.

499

500 **Acknowledgments**

501 This work was supported by the Brandenburg Ministry of Infrastructure and Agriculture (MIL),
502 who financed the land purchase, the Federal Agency for Renewable Resources (FNR), who co-
503 financed the AC system, and the interdisciplinary research project CarboZALF. The authors want
504 to express their special thanks to Mr. Peter Rakowski for excellent operational and technical
505 maintenance during the study period as well as to the employees of the ZALF research station,
506 Dedelow, for establishing and maintaining the CarboZALF-D field trial.

507

508 **References**



- 509 Alberti, G., Delle Vedove, G.D., Zuliani, M., Peressotti, A., Castaldi, S., Zerbi, G., 2010.
510 Changes in CO₂ emissions after crop conversion from continuous maize to alfalfa. *Agric.*
511 *Ecosyst. Environ.* 136, 139-147.
- 512 Baldocchi, D.D., 2003. Assessing the eddy covariance technique for evaluating carbon dioxide
513 exchange rates of ecosystems: past, present and future. *Glob. Change Biol.* 9, 479-492.
- 514 Batjes, N.H., van Wesemael, B., 2015. Measuring and monitoring soil carbon, in: Banwart, S. A.,
515 Noellemeyer, E., Milne, E. (Eds.), *Soil Carbon: Science, Management and Policy for*
516 *Multiple Benefits*. SCOPE Series 71. CABI, Wallingford, UK, pp. 188-201.
- 517 Berhe, A.A., Harte, J., Harden, J.W., Torn, M.S., 2007. The significance of the erosion-induced
518 terrestrial carbon sink. *BioScience* 57, 337-346.
- 519 Berhe, A.A., Kleber, M., 2013. Erosion, deposition, and the persistence of soil organic matter:
520 mechanistic consideration and problems with terminology. *Earth Surf. Processes*
521 *Landforms* 38, 908-912.
- 522 Bolinder, M.A., Kätterer, T., Andrén, O., Parent, L.E., 2012. Estimating carbon inputs to soil in
523 forage-based crop rotations and modeling the effects on soil carbon dynamics in a
524 Swedish long-term field experiment. *Can. J. Soil. Sci.* 92, 821-833.
- 525 Byrne, K.A., Kiely, G., Leahy, P., 2005. CO₂ fluxes in adjacent new and permanent temperate
526 grasslands. *Agric. For. Meteorol.* 135, 82-92.
- 527 Chen, L., Smith, P., Yang, Y., 2015. How has soil carbon stock changed over recent decades?
528 *Glob. Change Biol.* 21, 3197-3199.
- 529 Conant, R.T., Ogle, S.M., Paul, E.A., Paustian, K., 2011. Measuring and monitoring soil organic
530 carbon stocks in agricultural lands for climate mitigation. *Front. Ecol. Environ.* 9, 169-
531 173.



- 532 Culman, S.W., Snapp, S.S., Green, J.M., Gentry, L.E., 2013. Short- and long-term labile soil
533 carbon and nitrogen dynamics reflect management and predict corn agronomic
534 performance. *Agron. J.* 105, 493-502.
- 535 Davidson, E. A., Savage, K., Verchot, L. V., Navarro, R., 2002. Minimizing artifacts and biases
536 in chamber-based measurements of soil respiration. *Agric. For. Meteorol.* 113, 21-37.
- 537 De Gruijter, J.J., Brus, D.J., Bierkens, M.F.P., Knotters, M., 2006. Sampling for Natural
538 Resource Monitoring. Springer Verlag, Berlin.
- 539 Dobermann, A.R., Walters, D.T., Baker, J.M., 2006. Comment on “Carbon budget of mature no-
540 till ecosystem in north central region of the United States.” *Agric. For. Meteorol.* 136, 83-
541 84.
- 542 Doetterl, S., Berhe, A.A., Nadeu, E., Wang, Z., Sommer, M., Fiener, P., 2016. Erosion,
543 deposition and soil carbon: a review of process-level controls, experimental tools and
544 models to address C cycling in dynamic landscapes. *Earth Sci. Rev.* 154, 102-122.
- 545 Dymond, J.R., 2010. Soil erosion in New Zealand is a net sink of CO₂. *Earth Surf. Processes
546 Landforms* 35, 1763-1772. doi:10.1002/esp.2014.
- 547 Eickenscheidt, T., Freibauer, A., Heinichen, J., Augustin, J., Drösler, M., 2014. Short-term
548 effects of biogas digestate and cattle slurry application on greenhouse gas emissions
549 affected by N availability from grasslands on drained fen peatlands and associated organic
550 soils. *Biogeosciences* 11, 6187-6207.
- 551 Elsgaard, L., Görres, C., Hoffmann, C.C., Blicher-Mathiesen, G., Schelde, K., Petersen, S.O.,
552 2012. Net ecosystem exchange of CO₂ and carbon balance for eight temperate organic
553 soils under agricultural management. *Agric. Ecosyst. Environ.* 162, 52-67.
- 554 Foken, T., 2008. *Micrometeorology*. Springer Verlag, Berlin.



- 555 Ghimire, R., Norton, J.B., Pendall, E., 2014. Alfalfa-grass biomass, soil organic carbon, and total
556 nitrogen under different management approaches in an irrigated agroecosystem. *Plant Soil*
557 374, 173-184.
- 558 Gilmanov, T.G., Soussana, J.F., Aires, L., Allard, V., Ammann, C., Balzarolo, M., Barcza, Z.,
559 Bernhofer, C., Campbell, C.L., Cernusca, A., Cescatti, A., Clifton-Brown, J., Dirks,
560 B.O.M., Dore, S., Eugster, W., Fuhrer, J., Gimeno, C., Gruenwald, T., Haszpra, L.,
561 Hensen, A., Ibrom, A., Jacobs, A.F.G., Jones, M.B., Lanigan, G., Laurila, T., Lohila, A.,
562 Manca, G., Marcolla, B., Nagy, Z., Pilegaard, K., Pinter, K., Pio, C., Raschi, A., Rogiers,
563 N., Sanz, M.J., Stefani, P., Sutton, M., Tuba, Z., Valentini, R., Williams, M.L., Wohlfahrt,
564 G., 2007. Partitioning European grassland net ecosystem CO₂ exchange into gross
565 primary productivity and ecosystem respiration using light response function analysis.
566 *Agric. Ecosyst. Environ.* 121, 93–120.
- 567 Gilmanov, T.G., Wylie, B.K., Tieszen, L.L., Meyers, T.P., Baron, V.S., Bernacchi, C.J.,
568 Billesbach, D.P., Burba, G.G., Fischer, M.L., Glenn, A.J., Hanan, N.P., Hatfield, J.L.,
569 Heuer, M.W., Hollinger, S.E., Howard, D.M., Matamala, R., Prueger, J.H., Tenuta, M.,
570 Young, D.G., 2013. CO₂ uptake and ecophysiological parameters of the grain crops of
571 midcontinent North America: estimates from flux tower measurements. *Agric. Ecosyst.*
572 *Environ.* 164, 162–175.
- 573 Gomez-Casanovas, N., Anderson-Teixeira, K., Zeri, M., Bernacchi, C.J., DeLucia, E.H., 2013.
574 Gap filling strategies and error in estimating annual soil respiration. *Glob. Change Biol.*
575 19, 1941-1952.
- 576 Görres, C.-M., Kutzbach, L., Elsgaard, L., 2014. Comparative modeling of annual CO₂ flux of
577 temperate peat soils under permanent grassland management. *Agric. Ecosyst. Environ.*
578 186, 64–76.



- 579 Hernandez-Ramirez, G., Hatfield, J.L., Parkin, T.B., Sauer, T.J., Prueger, J.H., 2011. Carbon
580 dioxide fluxes in corn-soybean rotation in the midwestern U.S.: inter- and intra-annual
581 variations, and biophysical controls. *Agric. For. Meteorol.* 151, 1831-1842.
- 582 Hoffmann, M., Jurisch, N., Borraz, E.A., Hagemann, U., Drösler, M., Sommer, M., Augustin, J.,
583 2015. Automated modeling of ecosystem CO₂ fluxes based on periodic closed chamber
584 measurements: a standardized conceptual and practical approach. *Agric. For. Meteorol.*
585 200, 30-45.
- 586 Hollinger, S.E., Bernacchi, C.J., Meyers, T.P., 2005. Carbon budget of mature no-till ecosystem
587 in north central region of the United States. *Agric. For. Meteorol.* 130, 59-69.
- 588 IUSS Working Group WRB, 2015. World reference base for soil resources 2014. International
589 soil classification system for naming soils and creating legends for soil maps. Update
590 2015. *World Soil Resources Reports No. 106*. FAO, Rome.
- 591 Jans, W.W.P., Jacobs, C.M.J., Kruijt, B., Elbers, J.A., Barendse, S., Moors, E.J., 2010. Carbon
592 exchange of a maize (*Zea mays* L.) crop: influence of phenology. *Agric. Ecosyst.*
593 *Environ.* 139, 316-324.
- 594 Juszczak, R., Humphreys, E., Acosta, M., Michalak-Galczevska, M., Kayzer, D., Olejnik, J.,
595 2013. Ecosystem respiration in a heterogeneous temperate peatland and its sensitivity to
596 peat temperature and water table depth. *Plant Soil* 366, 505-520.
- 597 Kleber, M., Eusterhues, K., Keiluweit, M., Mikutta, C., Mikutta, R., Nico, P. S., 2015. Chapter
598 one – Mineral-Organic associations: Formation, Properties, and relevance in soil
599 environments. *Adv. Agro.* 130, 1-140.
- 600 Knebl, L., Leithold, G., Brock, C., 2015. Improving minimum detectable differences in the
601 assessment of soil organic matter change in short-term field experiments. *J. Plant Nutr.*
602 *Soil Sci.* 178, 35-42.



- 603 Koskinen, M., Minkkinen, K., Ojanen, P., Kämäräinen, M., Laurila, T., Lohila, A., 2014.
604 Measurements of CO₂ exchange with an automated chamber system throughout the year:
605 challenges in measuring night-time respiration on porous peat soil. *Biogeosciences* 11,
606 347-363.
- 607 Kutsch, W.L., Aubinet, M., Buchmann, N., Smith, P., Osborne, B., Eugster, W., Wattenbach, M.,
608 Schrupf, M., Schulze, E.D., Tomelleri, E., Ceschia, E., Bernhofer, C., Béziat, P.,
609 Carrara, A., Di Tommasi, P., Grünwald, T., Jones, M., Magliulo, V., Marloie, O.,
610 Moureaux, C., Olioso, A., Sanz, M.J., Saunders, M., Sørensen, H., Ziegler, W., 2010. The
611 net biome production of full crop rotations in Europe. *Agric. Ecosyst. Environ.* 139, 336-
612 345.
- 613 Kutzbach, L., Schneider, J., Sachs, T., Giebels, M., Nykänen, H., Shurpali, N.J., Martikainen,
614 P.J., Alm, J., Wilmking, M., 2007. CO₂ flux determination by closed-chamber methods
615 can be seriously biased by inappropriate application of linear regression. *Biogeosciences*
616 4, 1005-1025.
- 617 Lai, D.Y.F., Roulet, N.T., Humphreys, E.R., Moore, T.R., Dalva, M., 2012. The effect of
618 atmospheric turbulence and chamber deployment period on autochamber CO₂ and CH₄
619 flux measurements in an ombrotrophic peatland. *Biogeosciences* 9, 3305-3322.
- 620 Lal, R., Griffin, M., Apt, J., Lave, L., Morgan, G., M., 2004. Managing Soil carbon. *Science* 304,
621 393.
- 622 Langensiepen, M., Kupisch, M., van Wijk, M.T., Ewert, F., 2012. Analyzing transient closed
623 chamber effects on canopy gas exchange for flux calculation timing. *Agric. For.*
624 *Meteorol.* 164, 61-70.



- 625 Leiber-Sauheitl, K., Fuß, R., Voigt, C., Freibauer, A., 2013. High greenhouse gas fluxes from
626 grassland on histic gleysol along soil C and drainage grasslands. *Biogeosci. Discuss.* 10,
627 11283-11317.
- 628 Leifeld, J., Ammann, C., Neftel, A., Fuhrer, J., 2011. A comparison of repeated soil inventory
629 and carbon flux budget to detect soil carbon stock changes after conversion from cropland
630 to grasslands. *Glob. Change Biol.* 17, 3366-3375.
- 631 Leifeld, J., Bader, C., Borraz, E., Hoffmann, M., Giebels, M., Sommer, M., Augustin, J., 2014.
632 Are C-loss rates from drained peatlands constant over time? The additive value of soil
633 profile based and flux budget approach. *Biogeosci. Discuss.* 11, 12341-12373.
- 634 Livingston, G.P., Hutchinson, G.L., 1995. Enclosure-based measurement of trace gas exchange:
635 applications and sources of error, in: Matson, P.A., Harris, R.C. (Eds.), *Methods in
636 Ecology. Biogenic Trace Gases: Measuring Emissions from Soil and Water.* Blackwell
637 Science, Oxford, UK, pp. 14–51.
- 638 Lloyd, J., Taylor, J.A., 1994. On the temperature dependence of soil respiration. *Funct. Ecol.* 8,
639 315-323.
- 640 Luo, Y., Ahlström, A., Allison, S.D., Batjes, N.H., Brovkin, V., Carvalhais, N., Chappell, A.,
641 Ciais, P., Davidson, E.A., Finzi, A., Georgiou, K., Guenet, B., Hararuk, O., Harden, J.W.,
642 He, Y., Hopkins, F., Jiang, L., Koven, C., Jackson, R.B., Jones, C.D., Lara, M.J., Liang,
643 J., McGuire, A.D., Parton, W., Peng, C., Randerson, J.T., Salazar, A., Sierra, C.A., Smith,
644 M.J., Tian, H., Todd-Brown, K.E.O., Torn, M., van Groenigen, k.J., Wang, Y.P., West,
645 t.o., Wie, Y., Wieder, W.R., Xia, J., Xu, X., Xu, X., Zhou, T., 2016. Toward more
646 realistic projections of soil carbon dynamics by Earth system models. *Global
647 Biogeochem. Cycles* 30, 40-56.



- 648 Moffat, A.M., Papale D., Reichstein M., Hollinger, D.Y., Richardson, A.D., Barr, A.G.,
649 Beckstein, C., Braswell, B.H., Churkina, G., Desai, A.R., Falge, E., Gove, J.H., Heimann,
650 M., Hui, D., Jarvis, A.J., Kattge, J., Noormets, A., Stauch, V.J., 2007. Comprehensive
651 comparison of gap-filling techniques for eddy covariance net carbon fluxes. *Agric. For.*
652 *Meteorol.* 147, 209–232.
- 653 Necpálová, M., Anex Jr., R.P., Kravchenko, A.N., Abendroth, L.J., Del Grosso, S.J., Dick, W.A.,
654 Helmers, M.J., Herzmann, D., Lauer, J.G., Nafziger, E.D., Sawyer, J.E., Scharf, P.C.,
655 Strock, J.S., Villamil, M.B., 2014. What does it take to detect a change in soil carbon
656 stock? A regional comparison of minimum detectable difference and experiment duration
657 in the north central United States. *J. Soils Water Conserv.* 69, 517-531.
- 658 Paustian, K., Collins, H.P., Paul, E.A., 1997. Management controls on soil carbon, in: Paul, E.A.,
659 Paustian, K., Elliott, E.T., Cole, C.V. (Eds.), *Soil Organic Matter in Temperate*
660 *Agroecosystems: Long-Term Experiments in North America*. CRC Press, Boca Raton,
661 FL, pp. 15-50.
- 662 Poeplau, C., Bolinder, M.A., Kätterer, T., 2016. Towards an unbiased method for quantifying
663 treatment effects on soil carbon in long-term experiments considering initial within-field
664 variation. *Geoderma* 267, 41-47.
- 665 Pohl, M., Hoffmann, M., Hagemann, U., Giebels, M., Albiac Borraz, E., Sommer, M., Augustin,
666 J., 2014. Dynamic C and N stocks—key factors controlling the C gas exchange of maize in
667 a heterogeneous peatland. *Biogeosciences* 11, 2737-2752.
- 668 Reichstein, M., Falge, E., Baldocchi, D., Papale, D., Aubinet, M., Berbigier, P., Bernhofer, C.,
669 Buchmann, N., Gilmanov, T., Granier, A., Grünwald, T., Havránková, K., Ilvesniemi, H.,
670 Janous, D., Knohl, A., Laurila, T., Lohila, A., Loustau, D., Metteucci, G., Meyers, T.,
671 Miglietta, F., Ourcival, J.-M., Pumpanen, J., Rambal, S., Rotenberg, E., Sanz, M.,



- 672 Tenhunen, J., Seufert, G., Vaccari, F., Vesala, T., Yakir, D., Valentini, R., 2005. On the
673 separation of net ecosystem exchange into assimilation and ecosystem respiration: review
674 and improved algorithm. *Global Change Biol.* 11, 1424–1439.
- 675 Rieckh, H., Gerke, H.H., Sommer, M., 2012. Hydraulic properties of characteristic horizons
676 depending on relief position and structure in a hummocky glacial soil landscape. *Soil
677 Tillage Res.* 125, 123-131.
- 678 Saby, N.P.A., Bellamy, P.H., Morvan, X., Arrouays, D., Jones, R.J.A., Verheijen, F.G.A.,
679 Kibblewhite, M.G., Verdoodt, A., Üveges, J.B., Freudenschuß, A., Simota, C., 2008. Will
680 European soil-monitoring networks be able to detect changes in topsoil organic carbon
681 content? *Glob. Change Biol.* 14, 2432-2442.
- 682 Sainju, U.M., Singh, B.P., Whitehead, W.F., 2002. Long-term effects of tillage, cover crops, and
683 nitrogen fertilization on organic carbon and nitrogen concentrations in sandy loam soils in
684 Georgia, USA. *Soil Tillage Res.* 63, 167-179.
- 685 Savage, K.E., Davidson, E.A., 2003. A comparison of manual and automated systems for soil
686 CO₂ flux measurements: trade-offs between spatial and temporal resolution. *J. Exp. Bot.*
687 54, 891-899.
- 688 Schlichting, E., Blume, H.P., Stahr, K., *Soils Practical* (in German). Blackwell, Berlin, 1995.
- 689 Schrumpf, M., Schulze, E. D., Kaiser, K., Schumacher, J., 2011. How accurately can soil organic
690 carbon stocks and stock changes be quantified by soil inventories? *Biogeosciences* 8,
691 1193-1212.
- 692 Six, J., Conant, R.T., Paul, E.A., Paustian, K., 2002. Stabilization mechanisms of soil organic
693 matter: implications for C-saturation of soils. *Plant Soil* 241, 155-176.
- 694 Skinner, R.H., Dell, C.J., 2015. Comparing pasture C sequestration estimates from eddy
695 covariance and soil cores. *Agric. Ecosyst. Environ.* 199, 52-57.



- 696 Sommer, M., Augustin, J., Kleber, M., 2016. Feedbacks of soil erosion on SOC patterns and
697 carbon dynamics in agricultural landscapes – the CarboZALF experiment. *Soil Tillage*
698 *Res.* 156, 182-184.
- 699 Stewart, C.E., Paustian, K., Conant, R.T., Plante, A.F., Six, J., 2007. Soil carbon saturation:
700 concept, evidence and evaluation. *Biogeochemistry* 86, 19-31.
- 701 Stockmann, U., Padarian, J., McBratney, A., Minasny, B., de Brogniez, D., Montanarella, L.,
702 Hong, Y., S., Rawlins, B.G., Field, D.J., 2015. Global soil organic carbon assessment.
703 *Glob. Food Secur.* 6, 9-16.
- 704 Van Oost, K., Quine, T.A., Govers, G., De Gryze, S., Six, J., Harden, J.W., Ritchie, J.C.,
705 McCarty, G.W., Heckrath, G., Kosmas, C., Giraldez, J.V., da Silva, J.R., Merckx, R.,
706 2007. The impact of agricultural soil erosion on the global carbon cycle. *Science* 318,
707 626-629.
- 708 Van Wesemael, B., Paustian, K., Andr n, O., Cerri, C.E.P., Dodd, M., Etchevers, J., Goidts, E.,
709 Grace, P., K tterer, T., McConkey, B.G., Ogle, S., Pan, G., Siebner, C., 2011. How can
710 soil monitoring networks be used to improve predictions of organic carbon pool dynamics
711 and CO₂ fluxes in agricultural soils? *Plant Soil* 338, 247-259.
- 712 VandenBygaart, A.J., 2006. Monitoring soil organic carbon stock changes in agricultural
713 landscapes: issues and a proposed approach. *Can. J. Soil Sci.* 86, 451-463.
- 714 VandenBygaart, A.J., Gregorich, E.G., Helgason, B.L., 2015. Cropland C erosion and burial: is
715 buried soil organic matter biodegradable? *Geoderma* 239-240, 240-249.
- 716 Verma, S.B., Dobermann, A., Cassman, K.G., Walters, D.T., Knops, J.M., Arkebauer, T.J.,
717 Suyker, A.E., Burba, G.G., Amos, B., Yang, H., Ginting, D., Hubbard, K.G., Gitelson,
718 A.A., Walter-Shea, E.A., 2005. Annual carbon dioxide exchange in irrigated and rainfed
719 maize-based agroecosystems. *Agric. For. Meteorol.* 131, 77-96.



- 720 Wagle, P., Kakani, V.G., Huhnke, R.L., 2015. Net ecosystem carbon dioxide exchange of
721 dedicated bioenergy feedstocks: switchgrass and high biomass sorghum. *Agric. For.*
722 *Meteorol.* 207, 107-116.
- 723 Wang, K., Liu, C., Zheng, X., Pihlatie, M., Li, B., Haapanala, S., Vesala, T., Liu, H., Wang, Y.,
724 Liu, G., Hu, F., 2013. Comparison between eddy covariance and automatic chamber
725 techniques for measuring net ecosystem exchange of carbon dioxide in cotton and wheat
726 fields. *Biogeosciences* 10, 6865-6877.
- 727 Wehrhan, M., Rauneker, P., Sommer, M., 2016. UAV-based estimation of carbon exports from
728 heterogeneous soil landscapes - a case study from the CarboZALF experimental area.
729 *Sensors (Basel)* 16, 255.
- 730 Wuest, S., 2014. Seasonal variation in soil organic carbon. *Soil Sci. Soc. Am. J.* 78, 1442-1447.
- 731 Xiong, X., Grunwald, S., Corstanje, R., Yu, C., Bliznyuk, N., 2016. Scale-dependent variability
732 of soil organic carbon coupled to land use and land cover. *Soil Tillage Res.* 160, 101-109.
- 733 Yin, X., Goudriaan, J., Lantinga, E.A., Vos, J., Spiertz, H.J., 2003. A flexible sigmoid function of
734 determinate growth. *Ann. Bot.* 91, 361-371.
- 735 Yoo, K., Amundson, R., Heimsath, A.M., Dietrich, W.E., 2005. Erosion of upland hillslope soil
736 organic carbon: coupling field measurements with a sediment transport model. *Global*
737 *Biogeochem. Cycles* 19, 1-17.
- 738 Zan, C.S., Fyles, J.W., Girouard, P., Samson, R.A., 2001. Carbon sequestration in perennial
739 bioenergy, annual corn and uncultivated systems in southern Quebec. *Agric. Ecosyst.*
740 *Environ.* 86, 135-144.
- 741 Zeide, B., 1993. Analysis of growth equations. *For. Sci.* 39, 594-616.
- 742

743 **List of tables:**



744 **Tab. 1.:** Chamber-specific annual sums of CO₂ exchange (R_{eco} , GPP, NEE), $\text{NPP}_{\text{shoot}}$ and ΔSOC
745 (\pm uncertainty), as well as corresponding environmental variables measured during the study
746 period from 2010 to 2014.

747 **A.1.:** Management information regarding the study period from 2010 to 2014. Gray shaded rows
748 indicate coverage by chamber measurements.

749

750 **List of figures:**

751 **Fig. 1.:** Schematic representation of the study concept. Black stars represent SOC measured by
752 the soil resampling method. Black circles represent annual SOC derived using the C budget
753 method.

754 **Fig. 2.:** Transect of automatic chambers and chamber positions within the depression overlying
755 the Endogleyic Colluvic Regosol (WRB 2015, left). The black arrow shows the position of the
756 datalogger and controlling devices, which were placed within a wooden, weather-sheltered house.
757 The soil profile is shown on the right. Soil horizon-specific SOC (%) and Nt (%) contents are
758 indicated by solid and dashed vertical white lines, respectively. The high spatial variability in
759 ΔSOC and the basic principle of the C budget method are shown as the scheme within the
760 picture.

761 **Fig. 3.:** Time series of CO₂ exchange (A-D) for the four chambers of the AC system during the
762 study period from 2010 to 2014. R_{eco} (black), GPP (light gray) and NEE (dark gray) are shown as
763 daily sums (y-axis). NEE_{cum} is presented as a solid line, representing the sum of continuously
764 accumulated daily NEE values (secondary y-axis). The presented values display cumulative NEE
765 following soil manipulation to the end of 2014. Note the different scales of the y-axes. The grey



766 shaded area represents the period prior to soil manipulation. The dashed vertical line indicates the
767 soil manipulation. Dotted lines represent harvest events.

768 **Fig. 4.:** Time series of modeled aboveground biomass development (NPP_{shoot}) (A-D) for the four
769 chambers of the AC system during the study period from 2010 to 2014. NPP_{shoot} is shown as
770 cumulative values. The presented values display cumulative NPP_{shoot} following soil manipulation
771 to the end of 2014. The biomass model is based on biomass sampling (2010-2012) and biweekly
772 LAI measurements (2013-2014) during crop growth (grey dots). C removal due to chamber
773 harvests is shown by black dots. The grey shaded area represents the period prior to soil
774 manipulation. The dashed vertical line indicates the soil manipulation. Dotted lines represent
775 harvest events.

776 **Fig. 5.:** Temporal and spatial dynamics in cumulative ΔSOC throughout the study period based
777 on (A) the C budget method (measured/modeled; black lines) and (B) the soil resampling method
778 (linear interpolation; gray lines). The grey shaded area represents the period prior to soil
779 manipulation. The dashed vertical line indicates the soil manipulation. Dotted lines represent
780 harvest events. Temporal dynamics revealed by the C budget method allow for the identification
781 of periods being most important for the development of ΔSOC . Major spatial deviation occurred
782 during the maximum plant growth period (May to September). The proportion (%) of these
783 periods with respect to the standard deviation of estimated annual ΔSOC accounted for up to 79
784 %.

785 **Fig. 6.:** Average annual ΔSOC observed by soil resampling and the C budget method for (A) the
786 entire measurement site and (B) single chamber positions within the measured transect. ΔSOC
787 represents the change in carbon storage, with positive values indicating C sequestration and



788 negative values indicating C losses. Error bars display estimated uncertainty for the C budget
789 method and the analytical error of ± 5 % for the soil resampling method.

790 **A.3.:** Time series of recorded environmental conditions throughout the study period from 2010 to
791 2014. Daily Precipitation and GWL are shown for the upper (solid line) and lower (dashed line)
792 chamber position in the upper panel (A). The lower panel (B) shows the mean daily air
793 temperature. The grey shaded area represents the period prior to soil manipulation. The dashed
794 vertical line indicates the soil manipulation.

795

796

797

798

799

800

801

802

803

804

805



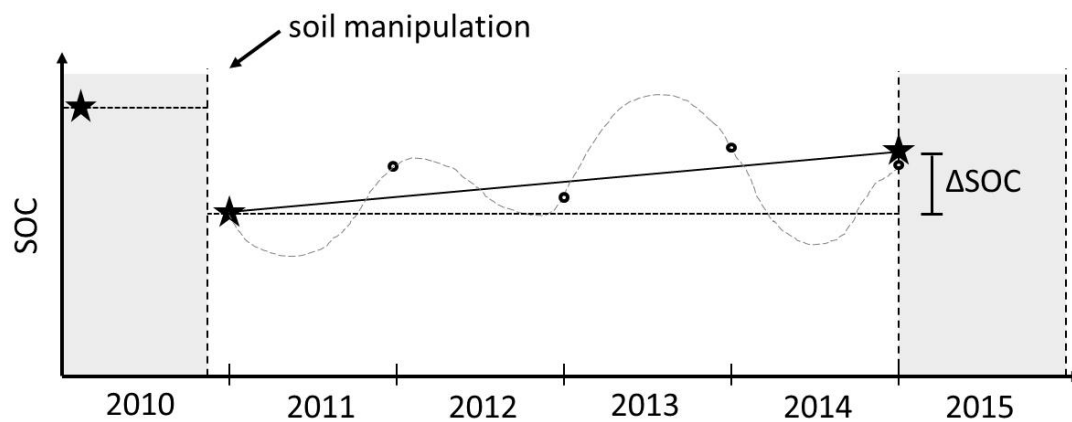
Tab.1

Year	Position	R _{eco}	GPP	NEE	ΔSOC	NPP _{shoot}		N	P	K	SOC to 1 m		NT to 1 m	NT in Ap	Precip.	GWL		
						harvested	modeled				depth	horizon					depth	horizon
			(g C m ⁻²)			(g m ⁻²)			(kg m ⁻² 0.3 m ⁻¹)		(kg m ⁻² 1 m ⁻¹)		(kg m ⁻² 0.3 m ⁻¹)		(mm)		(cm)	
2010	A (upper)	1014 ± 9	-1845 ± 8	-831 ± 12	-86 ± 66	744	745 ± 65	28.1	5.0	25.6	11.6	5.1	1.3	0.6		135		
	B (upper middle)	987 ± 11	-1970 ± 8	-983 ± 13	-251 ± 66	727	732 ± 64	24.7	4.1	18.0	9.1	4.2	0.9	0.4		103		
	C (lower middle)	1064 ± 38	-2000 ± 11	-935 ± 40	-190 ± 77	744	745 ± 65	25.5	4.2	16.9	9.1	4.2	0.9	0.4	516	95		
	D (lower)	1110 ± 21	-1737 ± 10	-627 ± 23	118 ± 69	744	745 ± 65	25.0	4.2	18.2	12.8	5.0	1.3	0.5		69		
2011	A (upper)	891 ± 13	-2022 ± 18	-1131 ± 22	149 ± 103	1238	1280 ± 101	29.5	5.4	30.2	10.5	3.5	1.1	0.4		129		
	B (upper middle)	855 ± 10	-1894 ± 13	-1039 ± 16	169 ± 96	1167	1208 ± 95	36.4	5.9	32.7	8.7	3.4	0.9	0.4		97		
	C (lower middle)	980 ± 14	-2062 ± 25	-1082 ± 28	79 ± 95	1115	1161 ± 91	33.7	5.6	32.9	9.0	3.7	0.9	0.4	618	87		
	D (lower)	843 ± 31	-1730 ± 8	-888 ± 32	59 ± 80	900	947 ± 73	35.0	5.7	31.8	12.2	4.0	1.3	0.4		61		
2012	A (upper)	1058 ± 86	-2659 ± 12	-1600 ± 87	-648 ± 104	297* / 634	952 ± 56	36.3	6.3	42.6						139		
	B (upper middle)	1075 ± 8	-2591 ± 11	-1516 ± 13	-472 ± 65	310* / 727	1044 ± 64	33.3	5.8	37.5						107		
	C (lower middle)	1286 ± 8	-2617 ± 9	-1331 ± 12	-346 ± 60	310* / 665	985 ± 59	32.7	5.4	35.5				585	87			
	D (lower)	1044 ± 10	-2194 ± 9	-1150 ± 13	-430 ± 39	299* / 420	720 ± 37	33.9	5.8	40.4						61		
2013	A (upper)	1140 ± 83	-1583 ± 9	-443 ± 83	-43 ± 91	290	400 ± 37	14.0	1.7	11.6						154		
	B (upper middle)	1283 ± 80	-1819 ± 8	-536 ± 80	-93 ± 86	304	443 ± 32	14.7	1.8	12.1						122		
	C (lower middle)	1438 ± 20	-1726 ± 7	-288 ± 22	107 ± 36	324	395 ± 29	15.6	1.9	12.9				499	94			
	D (lower)	1587 ± 80	-2036 ± 8	-448 ± 80	-6 ± 87	329	442 ± 34	15.9	2.0	13.2						68		
2014	A (upper)	1161 ± 15	-1615 ± 7	-455 ± 16	126 ± 26	605	581 ± 20	29.2	3.6	24.2	10.9	3.9	1.2	0.5		181		
	B (upper middle)	1443 ± 18	-2063 ± 7	-619 ± 19	-52 ± 28	635	567 ± 20	30.7	3.8	25.4	8.9	3.5	0.9	0.4		149		
	C (lower middle)	1683 ± 18	-2111 ± 6	-428 ± 19	36 ± 26	632	535 ± 18	30.5	3.8	25.3	9.0	3.7	0.9	0.5	591	121		
	D (lower)	1584 ± 12	-2113 ± 14	-528 ± 19	52 ± 28	587	580 ± 21	28.3	3.5	23.5	12.5	4.2	1.3	0.4		95		

* NPP_{shoot} is based on biomass samples collected next to each chamber because no chamber harvest was performed for winter fodder rye in 2012.



808 **Fig. 1**



809

810

811

812

813

814

815

816

817

818

819

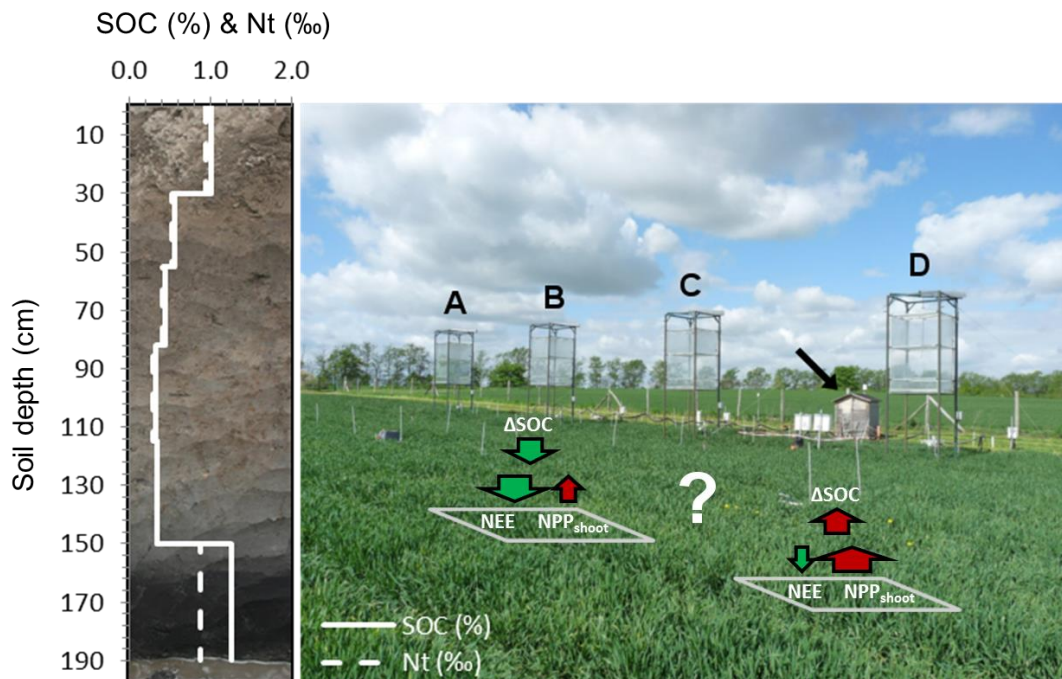
820

821

822

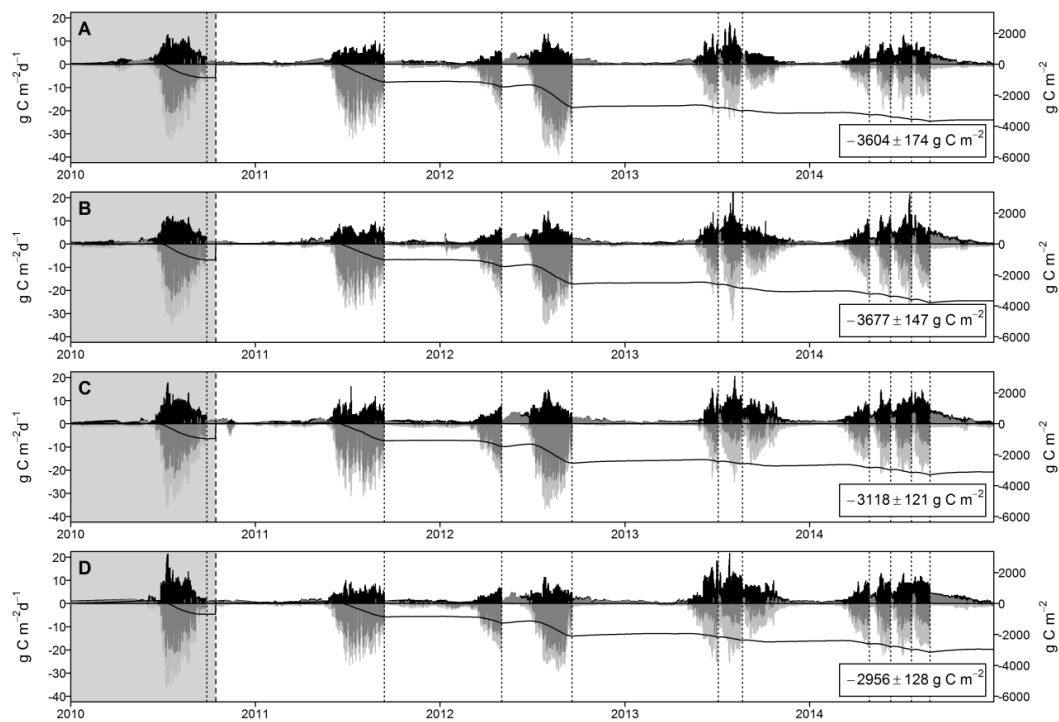


823 **Fig. 2**





834 **Fig. 3**



835

836

837

838

839

840

841

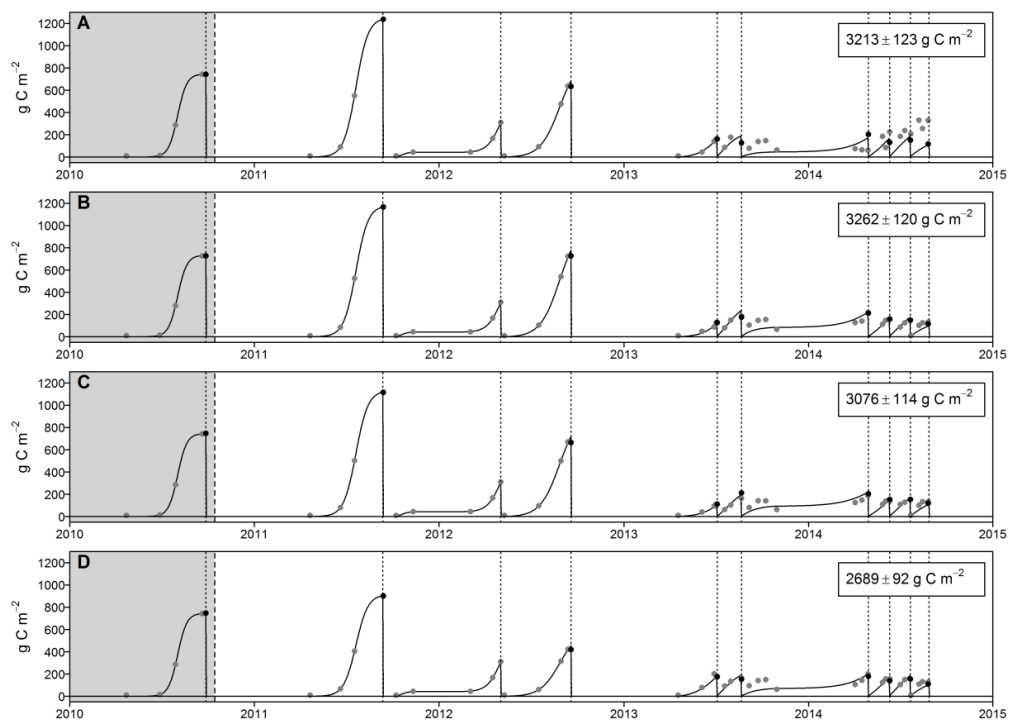
842

843

844



845 **Fig. 4**



846

847

848

849

850

851

852

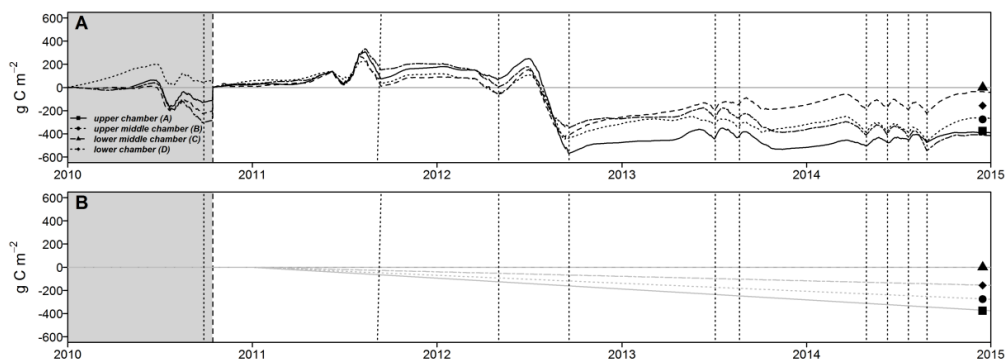
853

854

855



856 **Fig. 5**



857

858

859

860

861

862

863

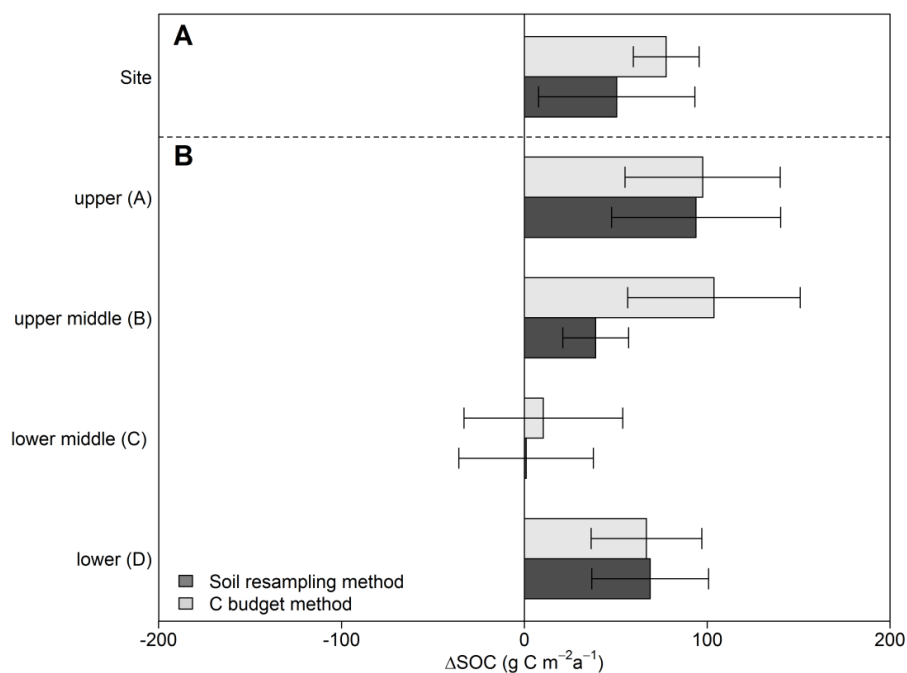
864

865

866



867 **Fig. 6**



868

869

870

871

872

873

874

875

876

877

878 **Appendices**879 **A.1**

Crop	Treatment	Details	Date
Winter fodder rye (<i>Secale cereale</i>)	Chamber dismounting		10/04/2010
	Herbicide application	Roundup (2 l/ha)	19/04/2010
	Fertilization	KAS (160 kg/ha N), 110 kg/ha P2O5, 190 kg/ha K2O, 22 kg/ha S and 27 kg/ha MgO	23/04/2010
	Ploughing	Chisel Plough	23/04/2010
Silage maize (<i>Zea mays</i>)	Sowing	10 seeds/m ²	23/04/2010
	Chamber installation		04/05/2010
	Herbicide application	Zintan Platin Pack	26/05/2010
Bare soil	Harvest		19/09/2010
	Chamber dismounting		20/09/2010
	Chamber installation		27/10/2010
	Chamber dismounting		05/04/2011
Silage maize (<i>Zea mays</i>)	Fertilization	110 kg/ha P2O5, 190 kg/ha K2O, 22 kg/ha S and 27 kg/ha MgO	06/04/2011
	Ploughing	Chisel Plough	21/04/2011
	Sowing	10 seeds/m ²	21/04/2011
	Herbicide application	Gardo Gold Pack, 3.5 l/ha	27/04/2011
	Fertilization	KAS (160 kg/ha N)	03/05/2011
	Chamber installation		04/05/2011
Bare soil	Harvest		13/09/2011
	Chamber dismounting		13/09/2011
	Ploughing	Chisel Plough	30/09/2011
Winter fodder rye (<i>Secale cereale</i>)	Sowing	270 seeds/m ²	30/09/2011
	Chamber installation		05/10/2011
	Fertilization	KAS (80 kg/ha N)	06/03/2012
	Harvest		02/05/2012
Bare soil	Chamber dismounting		02/05/2012
	Ploughing		08/05/2012
	Sowing	30 seeds/m ²	09/05/2012
Sorghum-Sudan grass (<i>Sorghum bicolor</i> x <i>sudanense</i>)	Fertilization	KAS (100 kg/ha N), Kieserite (100 kg/ha), 220 kg/ha P2O5, 190 kg/ha K2O	14/05/2012
	Chamber installation		22/05/2012
	Replanting		29/05/2012
	Herbicide application	Gardo Gold Pack (3 l/ha), Buctril (1.5 l/ha)	12/07/2012
	Harvest		18/09/2012
	Chamber dismounting		19/09/2012
Bare soil	Ploughing	Chisel Plough	09/10/2012
	Sowing	400 seeds/m ²	09/10/2012
	Chamber installation		19/10/2012
Winter triticale (<i>Triticosecale</i>)	Chamber dismounting		20/09/2012
	Chamber installation		17/10/2012
	Ploughing; fertilization	Chisel Plough; 44 kg/ha K2O, 48.4 kg/ha P40	15/04/2013
	Sowing	22 kg/ha	18/04/2013
Luzerne (<i>Medicago sativa</i>)	Harvest (first cut)		04/07/2013
	Fertilization	88 kg/ha K2O	10/07/2013
	Harvest (second cut)		21/08/2013
	Fertilization	200 kg/ha K2O, 110 kg/ha P2O5	27/02/2014
	Harvest (first cut)		29/04/2014
	Harvest (second cut)		10/06/2014
	Harvest (third cut)		21/07/2014
	Harvest (fourth cut)		27/08/2014
	Chamber dismounting		28/08/2014



880 **A.2 Weather and soil conditions**

881 A.3 shows the development of important environmental variables throughout the study period
882 (January 2010 – December 2014). In general, weather condition were similarly warm (8.7°C) but
883 also wetter (562 mm) compared to the long-term average (8.6°C; 485 mm). Temperature and
884 precipitation were characterized by distinct inter- and intra-annual variability. The highest annual
885 air temperature was measured in 2014 (9°C). The highest annual precipitation was recorded
886 during 2011 (616 mm). Lower annual mean air temperature and comparatively drier weather
887 conditions were recorded in 2010 (7.7°C; 515 mm) and 2013 (8.5°C; 499 mm). Clear seasonal
888 patterns were observed for air temperature. The daily mean air temperature at a height of 200 cm
889 varied between -18.8°C in February 2012 and 26.3°C in July 2010. Rainfall was highly variable
890 and mainly occurred during the growing season (55 % to 93 %), with pronounced heavy rain
891 events during summer periods, exceeding 50 mm d⁻¹. Despite a rather wet summer, only 67 mm
892 was measured in March and April 2012, the driest spring period within the study, resulting in late
893 germination and reduced plant growth. Annual GWL differed by up to 77 cm along the chamber
894 transect and followed precipitation patterns. Seasonal dynamics were characterized by a lower
895 GWL within the growing season (1.10 m) and enhanced GWL during the non-growing season
896 (0.85 m). From a short-term perspective, GWL was closely related to single rainfall events.
897 Hence, a GWL of 0.10 m was measured immediately after a heavy rainfall event in July 2011,
898 whereas the lowest GWL occurred during the dry spring in 2010. From August 2013 to
899 December 2014, the GWL was too low to apply the principal of hydrostatic equilibrium;
900 therefore, the groundwater table depth (> 235 cm) had to be used as a proxy.

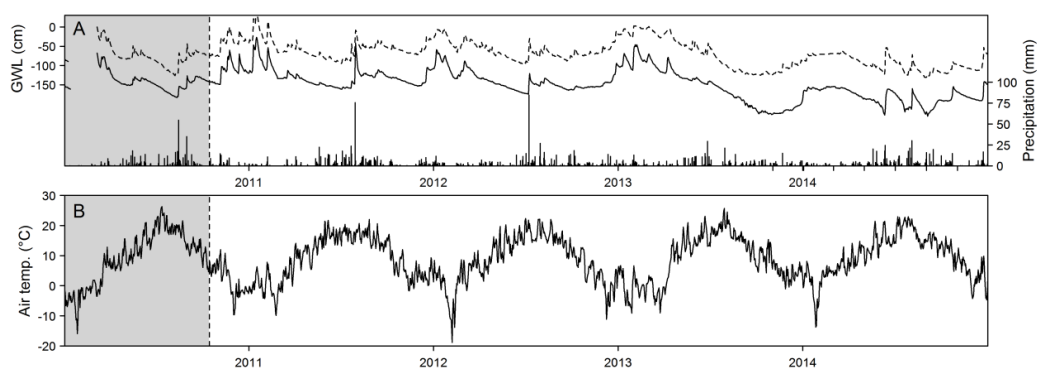
901

902

903



904 A.



905